

## Article

# Seismic Risk Assessment for the City of Sofia, Bulgaria

Dimcho Enchev Solakov <sup>\*ID</sup>, Dimitar Stefanov, Stela Simeonova and Plamena Raykova-Tsankova <sup>\*ID</sup>

National Institute of Geophysics, Geodesy and Geography—Bulgarian Academy of Sciences, 1113 Sofia, Bulgaria; dstefanov@geophys.bas.bg (D.S.); ssimeonova@geophys.bas.bg (S.S.)

\* Correspondence: dimos@geophys.bas.bg (D.E.S.); plamena.raikova@gmail.com (P.R.-T.)

**Abstract:** An earthquake is the most destructive natural phenomenon, with its sudden onset and rapid spread impacting large areas. Among the various geohazards, seismic ones dominate in terms of their social and economic effects on human life and the urban environment. In the present study, a deterministic earthquake ground motion scenario for the city of Sofia (the capital of Bulgaria) is presented. The earthquake risk posed to Sofia is quantified by considering the city's seismic context, which contributes to its hazard and risk. The assessment of seismic hazards and the generation of earthquake scenarios make up the first step of seismic risk evaluations, as risk reduction strategies can only be developed with a better understanding of these threats. Risk assessment and its associated management comprise the most effective approach to estimating the impact of seismic hazards on the city of Sofia, which exhibits high seismic activity. Our findings provide a basis for local governments to review their susceptibility and preparedness. The consideration of earthquake scenarios in the creation of policies for seismic risk reduction will allow us to focus on the prevention of earthquake effects rather than on the activities following these disasters.

**Keywords:** geohazard; seismic hazard; seismic risk; building stock; city of Sofia; Bulgaria



**Citation:** Solakov, D.E.; Stefanov, D.; Simeonova, S.; Raykova-Tsankova, P. Seismic Risk Assessment for the City of Sofia, Bulgaria. *Geosciences* **2024**, *14*, 307. <https://doi.org/10.3390/geosciences14110307>

Academic Editors: Hans-Balder Havenith, Maksim Bano, Mohammed Farfour and Nikos Economou

Received: 30 August 2024

Revised: 15 October 2024

Accepted: 6 November 2024

Published: 13 November 2024



**Copyright:** © 2024 by the authors. Licensee MDPI, Basel, Switzerland. This article is an open access article distributed under the terms and conditions of the Creative Commons Attribution (CC BY) license (<https://creativecommons.org/licenses/by/4.0/>).

## 1. Introduction

Sofia is Bulgaria's capital and largest city, the country's most industrial and cultural region, and a typical example of an area with high seismic risk.

Sofia's history spans thousands of years, from antiquity to modern times, during which the city was a commercial, industrial, cultural, and economic center in its region and the Balkans.

In the New Stone Age (Neolith), VI–V century BC, there were numerous prehistoric settlements located in the Sofia Valley, the closest one being today's neighborhood of Slatina. This epoch and settlement mark the beginning of the historical city center of Sofia, which has not changed its location to this day. Its new name, Sredets, is associated with the period of the First Bulgarian Empire, during which it developed into an important political, military, economic, and cultural center for almost two centuries [1]. During the Second Bulgarian Empire, the city experienced prolonged economic and cultural prosperity, growing and finally looking like a typical medieval city: the streets narrowed, buildings with characteristic brick–stone structures appeared, new small churches were erected, and many monasteries appeared in the vicinity, mostly on the slopes of Vitoshka and Stara Planina. In the final decades of the XIV century, the city began to be called by its present name—Sofia. In 1879, the first urban development plan of Sofia was drawn (presented in Figure 1a) [1], transforming the city's skyline and largely shaping today's city center. Some of the most prominent architects and builders were recruited for the construction of the new capital. In 1888, Sofia occupied an area of 2.49 km and held a population of 30,428 people, reaching 6.64 km and 86,787 inhabitants in 1907 [1]. Currently, Sofia is the largest city in Bulgaria (Figure 1b), with 1,286,965 residents, ranking as the 14th largest city in the European Union.

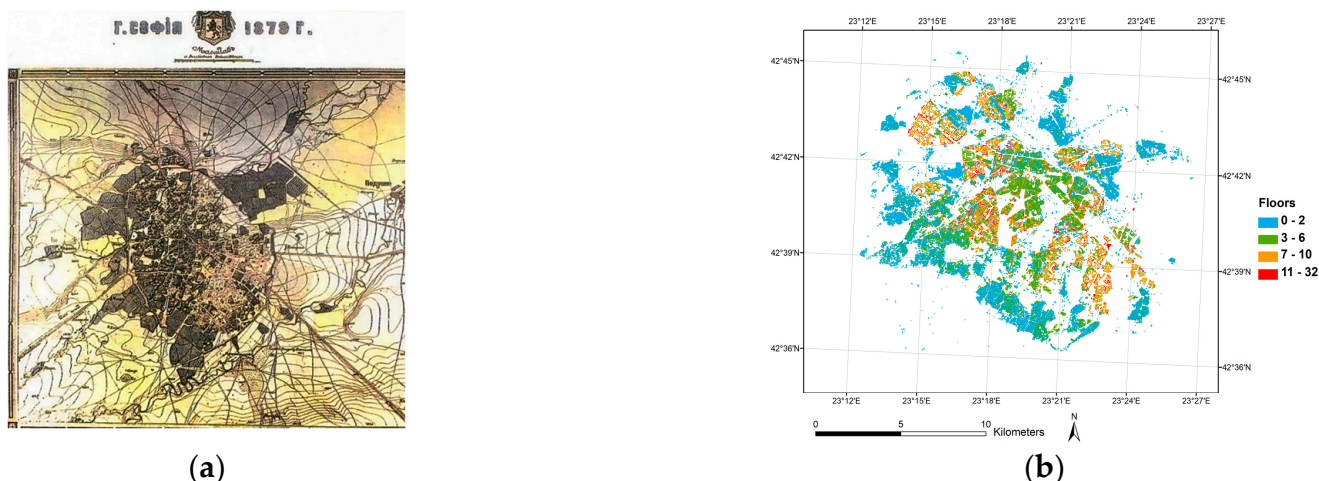


**Figure 1.** City of Sofia: (a) first urban development plan from 1879 and (b) current building distribution by floor number.

At present, Sofia is Bulgaria's economic hub and home to most major national and international companies operating in the country, as well as local universities and other cultural institutions.

The city is situated in Western Bulgaria, at the northern foothills of the Vitosha Mountain, in the Sofia Valley, surrounded by the Balkans to the north and the Vitosha and Lyulin Mountains to the south and west, respectively.

The city is located in the Sofia seismogenic zone, encompassing the area around the NWW-SEE-trending Sofia graben, a region characterized by medium-speed horizontal movements. Indeed, the region's contemporary tectonic activity is predominantly associated with the marginal faults of this graben [2].

Our study focuses on the geohazard associated with earthquake generation and its socioeconomic effects on human life and the urban environment.

A deterministic seismic scenario for Sofia (represented as macroseismic intensity, MSK) is presented, with magnitude  $M_W 6.5$ , reproducing the "true" historical 1858 earthquake, which had the strongest seismic impact on the city and originated from the active fault along the northern margin of the Vitosha Mountain.

Sofia's deterministic local ground-shaking representation is produced through a GIS by combining the location of the earthquake scenario with the assigned magnitude, the appropriate attenuation relations for the selected ground motion descriptor, and a seismically oriented geological/geotechnical zonation of the urban area.

The approach adopted in the Risk EU Project (2001–2004) funded by The European Economic Commission in the framework of the Fifth Research and Technological Development Program "Energy, Environment and Sustainable Development" (presented in [3,4]) was used to generate the deterministic seismic scenario in question.

The consideration of seismic risk scenarios will help the local government prepare response plans for natural disasters.

## 2. Materials and Methods

### 2.1. Deterministic Earthquake Scenario for the City of Sofia

The work on deterministic seismic scenarios was guided by the ultimate goal of producing a usable and realistic ground motion map for the urban area.

#### 2.1.1. Seismotectonics

The tectonic situation in the Eastern Mediterranean and Balkans is dominated by the collision of the Arabian and African plates with the Eurasian one (among others [5]). Bulgaria's recent tectonics have been determined by the region's geotectonic conditions, dominated by north–south extension processes [6]. Recent studies show that Central

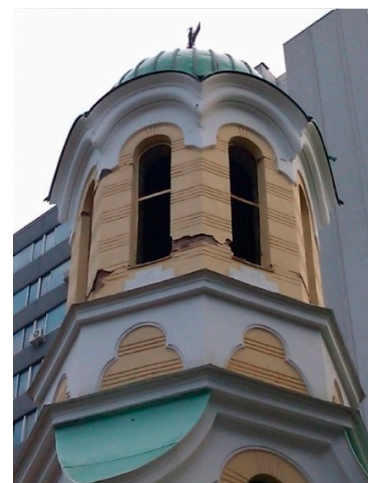
Western and Southwestern Bulgaria belong to the South Balkan Extensional Region, a transition zone between the Eurasian continental plate and the Aegean micro-plate [6].

The available historical documents prove the occurrence of destructive earthquakes during the 15th–18th centuries in this area. Prior to the 19th century, Sofia was a small town, nestled in the Ottoman Empire, presenting few reports on earthquakes felt in the region. The first well-documented strong earthquake occurred on 4 April 1818, with  $I_0 = 8\text{--}9$  MSK [7] and  $M_W 6.0$ , near Sofia [8]. The strongest documented event that occurred in Sofia's seismogenic zone took place on the 18/30 September 1858, with magnitude  $M_W 6.5$  and a maximum epicentral intensity of  $I_0 = 9\text{--}10$  MSK. This earthquake was felt in Southern and Southwestern Bulgaria and Northern Greece. Out of the twenty-eight mosques and seven churches in Sofia, only three of the former and two of the latter remained unaffected and functioning. The water flow of the hot springs in the town center decreased before the earthquake and stopped for 24 h afterward, a new water spring appearing in the southwestern part of Sofia [8].

During the 20th century, the strongest event that occurred in the vicinity of Sofia was the 1917 earthquake, with  $M_W 5.7$  ( $I_0 = 7\text{--}8$  MSK), causing several instances of moderate damage (Figure 2a) and changing the capacity of the thermal mineral springs in Sofia and its surroundings. This earthquake was felt for 50,000 km<sup>2</sup> and was followed by aftershocks for more than a year [2].



(a)



(b)

**Figure 2.** Damages caused by the (a) 1917  $M_W 5.7$  and (b) 2012  $M_W 5.6$  earthquakes.

Almost a century later, an earthquake with  $M_W 5.6$  hit Sofia's seismic zone, on 22 May 2012. This earthquake was located around 25 km southwest of Sofia, near the city of Pernik. Moderate to heavy damage was observed in the epicentral area, spanning Pernik, Radomir, and Sofia (Figure 2b). The event was largely felt around Bulgaria and in neighboring countries, including Northern Greece, Eastern North Macedonia, Eastern Serbia, and Southern Romania. The aftershock activity lasted about 2 years [9].

The regional seismicity pattern is concentrated mainly in the upper 10–15 km of the Earth's crust [10], as illustrated in Figure 3, representing the epicenter map of historical and instrumental (after the introduction of a modern seismic network in Bulgaria) earthquakes in Sofia's seismogenic zone. This figure also displays the active faults defined in [11].

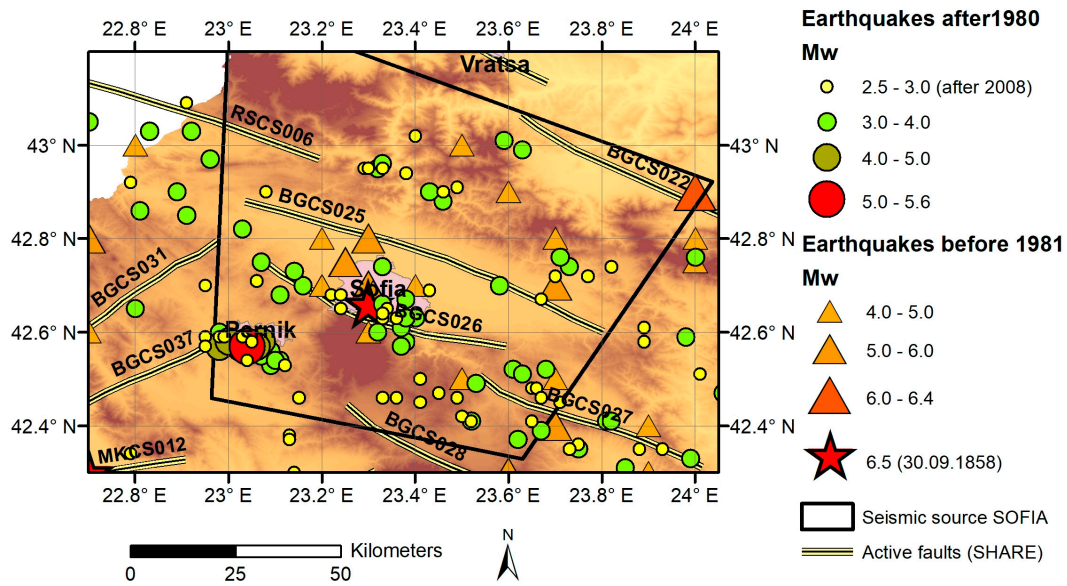


**Figure 3.** Spatial seismic patterns (historical and instrumental—after 1981—earthquakes with  $M_w > 3.0$ ) and tectonic map for Sofia and its surroundings.

### 2.1.2. Soil Properties

The city’s soil properties were represented through the engineering parameter  $V_{s30}$ —the average shear-wave velocity in the upper 30 m of the soil/rock profile—the values (illustrated in Figure 4) based on the results in [6,12] and supplemented with USGS slope-based global model data (available at <https://earthquake.usgs.gov/data/>, (accessed on 30 August 2024)) for the city’s built-up area. The figure below illustrates variations in  $V_{s30}$  values from 170 to 1100 m/s, whereby the highest ones are located around the Vitosha Mountain and the lowest ones are in the southern parts of the city, directly under it.

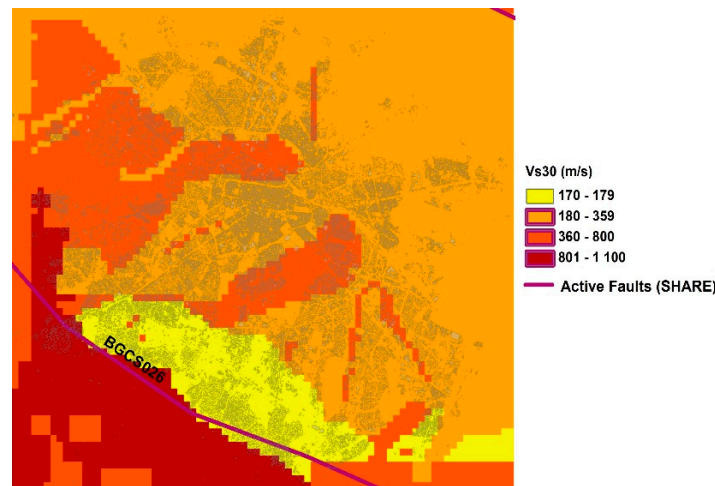


**Figure 4.** Average shear-wave velocity in the upper 30 m of the soil/rock profile of Sofia.

### 2.1.3. Ground Motion Attenuation (GMPEs)

Selecting appropriate ground motion prediction equations (GMPEs, also known as attenuation relations or models) is essential for seismic hazard assessment and requires the definition of tectonic setting-related criteria, basic dataset characteristics, prediction equation frequency ranges, and other factors. Details on the selection and justification of ground motion prediction equations are presented in [6].

For the Sofia area, six ground motion models for tectonically active regions were selected: AS14 [13], AB14 [14], BA14 [15], CB14 [16], CY14 [17], and CF15 [18].

The method presented in [19] was chosen to test the six models selected against real ground motion data from Italy and Balkan and Middle Eastern countries, derived from the engineering strong motion (ESM) model presented in [20]. The fit between the observed data and the model results is given by the following equation:

$$LLH = -\frac{1}{N} \sum_{i=1}^N \log_2(g(x_i)), \quad (1)$$

where  $N$  is the number of observations  $x_i$ , and  $g$  is the probability density function predicted by the GMPEs (normal distribution). A small  $LLH$  value (ranking criterion) indicates a high similarity of the candidate model to the observational one.

The approach presented in [21] was used to weight the selected GMPEs, later used in the probabilistic earthquake scenarios.

#### 2.1.4. Deterministic Seismic Scenario

Importantly, our approach requires the deterministic scenario to be consistent with the regional seismotectonics, the city's seismic history, and the active faults that have generated the earthquakes with the largest macroseismic impacts on the urban area considered.

This study's scenario featured the "true" historical 1858  $M_W$ 6.5 earthquake, which had the strongest seismic impact on Sofia and originated from the active fault along the northern margin of the Vitosha Mountain. At present, this fault demonstrates displacement of earth's surface according to SAR data [22,23]. The ground motion along the city was estimated by applying the six selected GMPEs for an active, shallow crustal tectonic regime.

Sofia's deterministic ground motion scenario for a macroseismic intensity of I MSK is mapped in Figure 5.

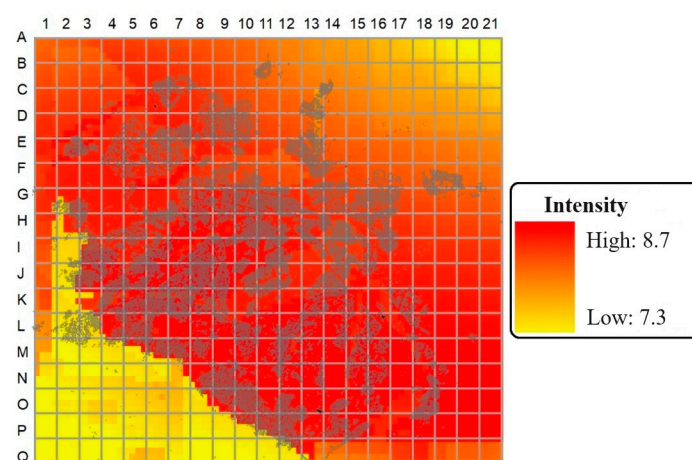


**Figure 5.** The deterministic earthquake scenario for  $M_W$ 6.5 in terms of a macroseismic intensity of I MSK.

The highest intensity values (up to 8.7 MSK) were in the southwestern part of the city, close to the northern margin of the Vitosha Mountain.

#### 2.1.5. Seismic Risk Assessment Methodology

A GIS-based methodology for national-scale seismic risk assessment was developed and applied to Bulgaria. This was grounded in the "Methodology for Analysis, Evaluation and Mapping of the Seismic Risk of the Republic of Bulgaria", developed by the NIGGG-BAS for the Ministry of Regional Development and Public Works and approved by the Minister, having the force of a normative document [24]. More specifically, the methodology was based on the application of empirical methods for determining buildings' vulnerability using the EMS-98 approach [25].

The first step comprised identifying regions with equal macroseismic intensity, referring to the seismic intensity map. Then, each building was assigned to a relevant vulnerability class following an EMS-based procedure, from A to F. For each group, the number of buildings reaching a certain damage grade was calculated directly using DPM (damage probability matrix) values for the vulnerability class, depending on their location's seismic intensity. Among all buildings in the region with the same intensity and vulnerability class, those with an equal damage grade were selected to determine the number of damaged structures. Subsequently, the area of damaged buildings according to their damage grades was also calculated from the regional GIS database and then used to assess monetary losses and human casualties. This methodology requires all information to be available in a GIS system and individually applied to each elementary cell of the region's GIS representation.

## 2.2. Building Stock Identification and Classification

### 2.2.1. Building Stock Database

Sofia is a city with a rich architectural heritage, including Roman, Byzantine, and medieval Bulgarian buildings, which was combined, at the start of the 20th century, with national architectural features, forming a new style—the national romantic Bulgarian Secession.

The building stock varies in terms of the year and period of design and construction, as well as the period already in use compared to the normalized service life.

The structure of the modern cadaster and property registry system, including its format and specifics, was thus chosen for the subsequent processing and assessment of hazards, with the following main parameters: structural system (structure), year of construction, floor plan, functional purpose, and expanded built-up area.

Regarding the spatial distribution of building types over the years, the oldest preserved residential buildings are located in the city's historic center. During the communist regime (1944–1989), residential blocks were mass-built, according to industrial systems (large-area formwork and large-panel buildings), forming new neighborhoods in the outskirts of the city. After the establishment of the democratic system (in 1990), large-panel buildings were mainly replaced by monolithic reinforced concrete buildings.

All input information for the building stock was obtained from the Bulgarian state Geodesy, cartography and cadastre agency. Each building had its own identification number and contained the parameters necessary for the analysis. There were also cases with incomplete information for which a visual inspection had to be carried out.

In the present study, only residential buildings were considered, totaling 91,002 structures for a total built-up area of 67,744,515 m<sup>2</sup>.

To correctly process Sofia's building stock input data, a grid (930 m × 1045 m) was imposed, as presented in Figure 6, its dimensions specifically chosen to correspond to that of a geographical map of the city on a scale of 1:19,000 (100 × 70 cm). This was necessary to facilitate building localization and, if necessary, perform specific visual inspections.

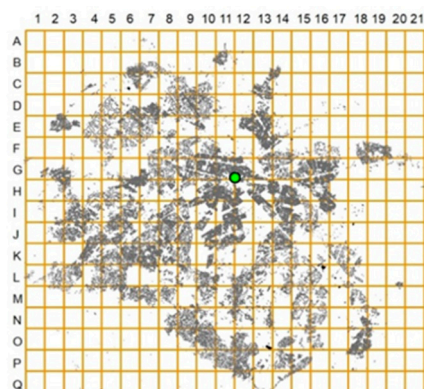


**Figure 6.** Network imposed on the input data for Sofia's building stock.

### 2.2.2. Building Stock Classification

The classification of the building stock was carried out based on three parameters—number of floors, year of construction, and type of structure (typology)—and this information is from Sofia’s cadastral map (obtained from the Bulgarian state agency for geodesy, cartography, and cadaster).

The distribution of buildings (in numbers and total floor area [m<sup>2</sup>] (TFA)) by height, sorting them into four groups, is shown in Table 1. Most of the buildings (71,187) can be classified as low-rise, with up to 3 floors, while 10,801 buildings are in the range of 4 to 6 floors, 7706 buildings are in the range of 7 to 9 floors, and only 1308 buildings are above 10 floors. Low-rise buildings are extremely numerous—78% of all buildings, but their area is only 14.7% of the total area. Medium-tall buildings (between 7 and 9 floors) are only 8.5% in number, but their total built-up area is the largest—42.7%. Tall buildings are only 1.5% in number, but their area is about 18%.

**Table 1.** Distribution of buildings (number and total floor area in [m<sup>2</sup>]) by number of floors.

Floors	1 to 3	4 to 6	7 to 9	Above 10
Number	71,187	10,801	7706	1308
%	78.2	11.9	8.5	1.4
TFA [m <sup>2</sup> ]	9,984,240	16,952,445	28,945,612	11,862,218
%	14.7	25.0	42.7	17.6

An important building stock parameter is the design year (construction), directly related to the design seismic codes prevalent in that period. Bulgarian national seismic codes are periodically updated and modernized, the timing of which also sets boundaries between time periods. In this case, seven time periods were considered.

Table 2 shows the distribution of buildings by construction period. Most buildings (19,685) were built in 1966–1977, but maximum TFA coverage was seen after 2007, following a continuous growth trend, clearly showing the city’s sustainable rate of development over time.

**Table 2.** Distribution of number of buildings and total floor area [m<sup>2</sup>] by construction period.

Period	Until 1929	1930–1957	1958–1965	1966–1977	1978–1987	1988–2007	After 2007
Number	2725	12,729	19,446	19,685	14,812	10,479	11,126
%	3.0	14.0	21.4	21.6	16.3	11.5	12.2
TFA [m <sup>2</sup> ]	273,052	2,084,714	4,528,991	10,449,994	14,700,537	15,836,844	19,870,383
%	0.4	3.1	6.7	15.4	21.7	23.4	29.3

Based on the cadaster design system information, each building was classified in a separate type according to the typological matrix of Bulgarian buildings, with eight typologies in total. Some of them are shown in Figure 7.

The distribution of buildings by typologies (number of buildings) is presented in Table 3.

**Table 3.** Distribution of buildings by typologies (number of buildings).

Type	M1	M2	RC1	RC2	RC4	RC5	RCp6	RCp7
Pcs.	47,552	15,203	17,525	3844	1078	748	90	4962
%	52.3	16.7	19.3	4.2	1.2	0.8	0.1	5.5



**Figure 7.** Building typologies in Sofia: (a) five-story masonry building with reinforced concrete belts, type M1; (b) three-story masonry house with wooden beams, type M2; (c) skeletal beamless reinforced concrete structure, type RC2; (d) structures with reinforced concrete shear walls, type RC4; (e) reinforced concrete structure with shear walls and columns, type RC5; and (f) six-story large-panel building, type RCp7.

Most buildings (47,552) fell into the M1 typology (masonry structures, unreinforced masonry with reinforced concrete slabs, beams, and belts, not framed or framed by columns). The RC1 typology (concrete frame structures) ranked second, with 17,525 buildings, followed by M2 (massive masonry structures with wooden beams), totaling 15,203 units; meanwhile, large-panel buildings (RCp7) ranked fourth, with only 4962 structures. Masonry structures (M1 and M2) accounted for over half of all buildings (69%).

The typological distribution of buildings (total floor area) was quite different, as shown in Figure 8: reinforced concrete structures (RC1) dominated, covering 28.3% of the total area, followed by reinforced concrete structures (RC2, skeletal beamless), occupying 22.1%, and large-panel buildings (RCp7), accounting for 10.3%. The overall area occupied by masonry structures (M1 and M2) only amounted to 13.4% of the total.



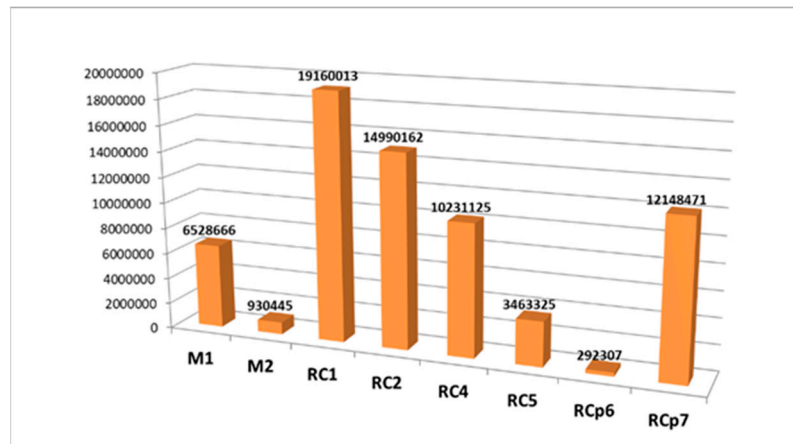


Figure 8. Distribution of buildings by typologies (total floor area [m<sup>2</sup>]).

### 2.2.3. Building Stock Seismic Vulnerability Assessment

A seismic vulnerability assessment was performed for each building individually, based on information on its load-bearing structure (typology), construction time (design), number of floors, and other technical parameters, assigning each unit a corresponding vulnerability class. The results obtained are illustrated in Figures 9 and 10, displaying the distribution of buildings by number and TFA (total floor area [m<sup>2</sup>]).

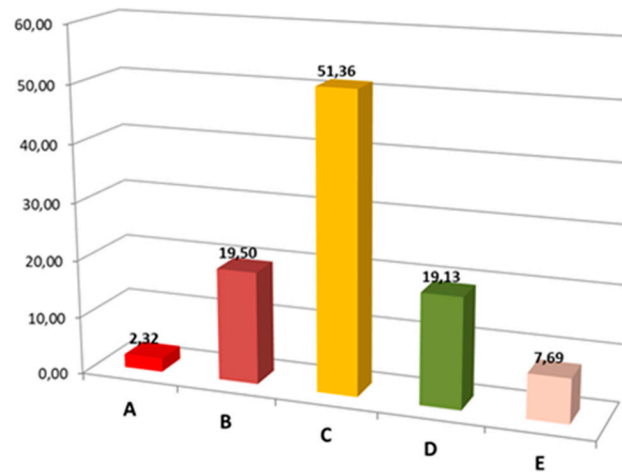


Figure 9. Number of buildings (%) in the various vulnerability classes.

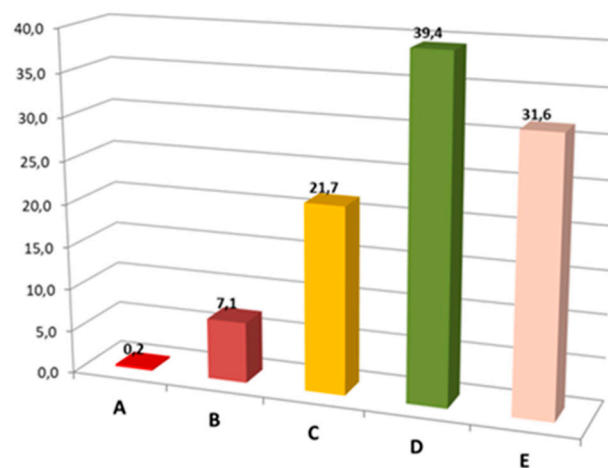


Figure 10. Total floor area (%) in vulnerability classes.

Most buildings fell into class “C”, amounting to 51.3%. In second and third place were class “B” and “D” buildings, totaling 19.5% and 19.1%, respectively. In terms of the total built-up area, class “D” again dominated with 39.4%, followed by class “E”, with 31.6%. The most radical difference is class “C” with 21.7% (at 51.3% by number of buildings).

Figures 11 and 12 show the distribution of buildings by predominant vulnerability class.

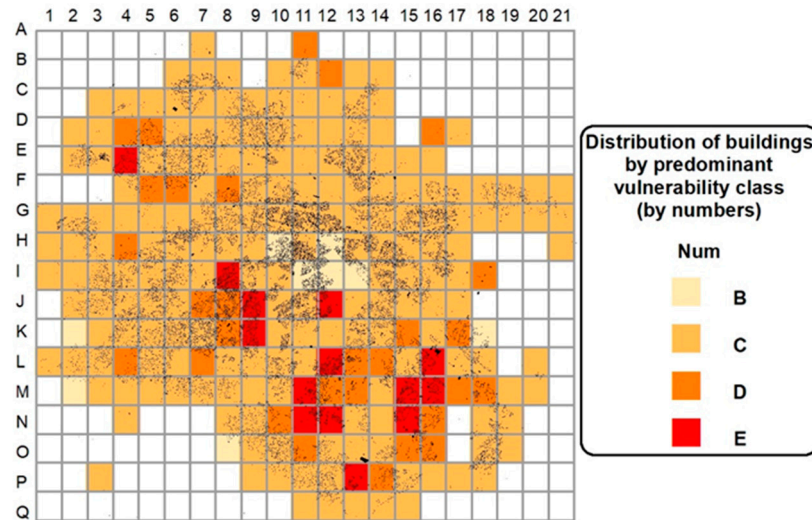


Figure 11. Distribution of buildings (number) by predominant vulnerability class.

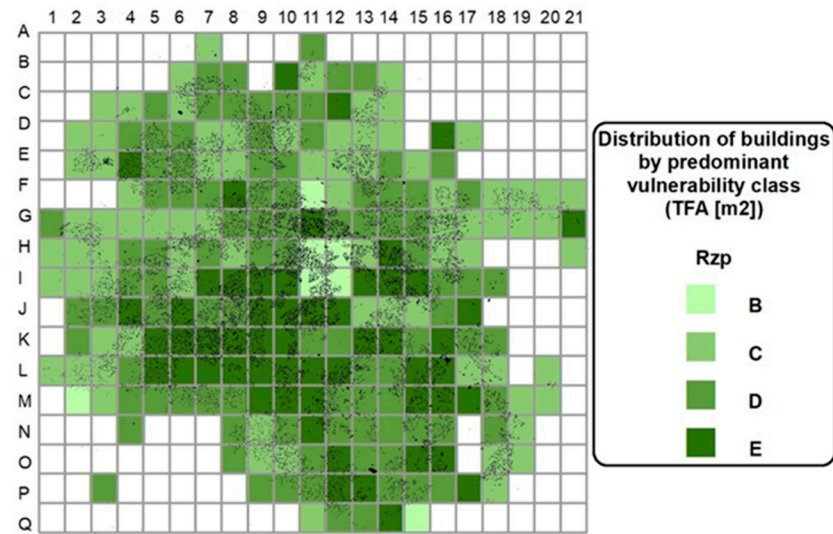


Figure 12. Distribution of buildings (TFA [m<sup>2</sup>]) by predominant vulnerability class.

### 3. Results

#### 3.1. Seismic Risk Assessment

##### 3.1.1. Direct Damages and Destruction

Based on the information collected regarding the building stock and the conducted analysis, we assessed the direct damages and destruction, following the algorithms and criteria detailed in the Methodology Section [24]. The distribution of buildings by number and total floor area (TFA [m<sup>2</sup>]), split between different damage levels, is summarized in Table 4, where their distribution as a percentage of the total number and built-up area is also shown.

**Table 4.** Distribution of buildings (by number and TFA) with different damage levels.

Damage Grade/	No Damage	Slight	Medium	Heavy	Very Heavy	Destruction
Number of buildings	18,993	25,891	22,652	14,728	6903	1835
Number of buildings in (%)	20.87	28.45	24.89	16.18	7.59	2.02
Total floor area in [m <sup>2</sup> ]	25,999,587	21,893,338	12,010,190	5,372,247	2,035,016	434,137
Total floor area in (%)	38.38	32.32	17.73	7.93	3.00	0.64

The built-up area of buildings without and with slight damage is 38.4% and 32.3%, respectively. The buildings with medium damage are next—17.7%. High damage rates are relatively low at 7.93% for heavy and 3.0% for very heavy damage. The area of destroyed buildings is minimal—0.64%. Figures 13–16 illustrate some of the obtained results. The most significant damage is observed in those parts of the city where the oldest low-rise buildings are located. The presence of old buildings with a higher vulnerability and on the other a very high seismic intensity ( $I = 8.6$  to  $I = 8.8$ ).

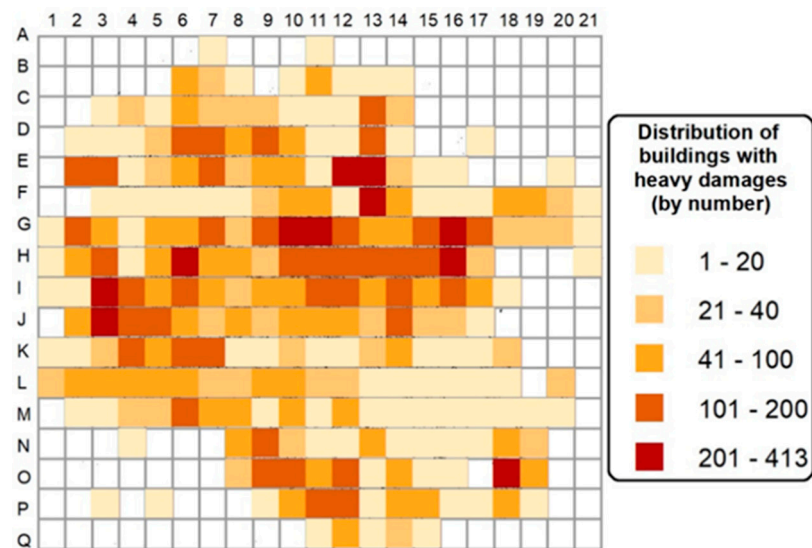


**Figure 13.** Distribution of buildings with heavy damages—by numbers.

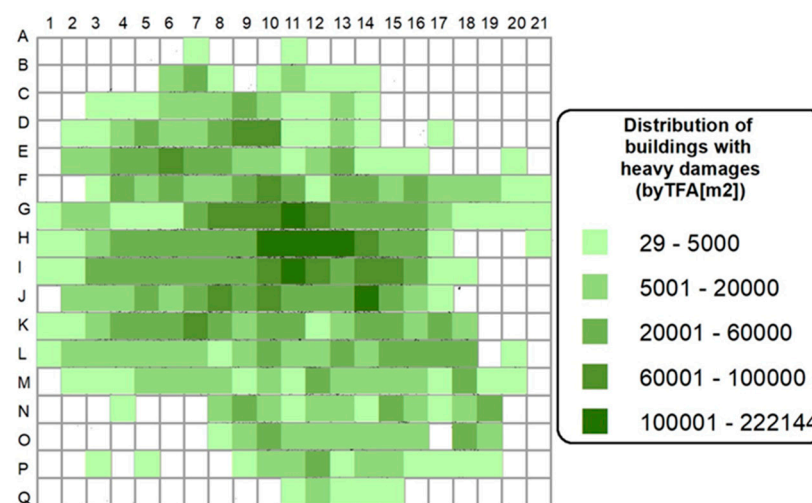


**Figure 14.** Distribution of buildings with heavy damages—TFA [m<sup>2</sup>].

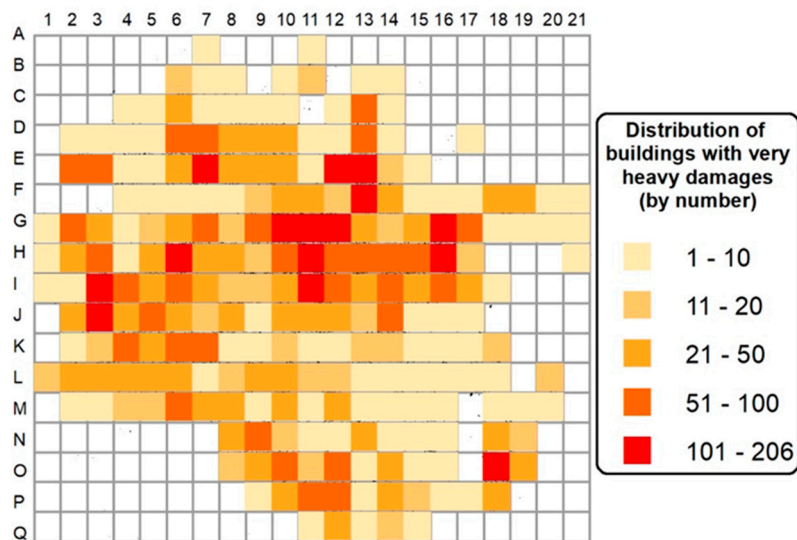


Figure 15. Distribution of buildings with very heavy damages, based on—by numbers.

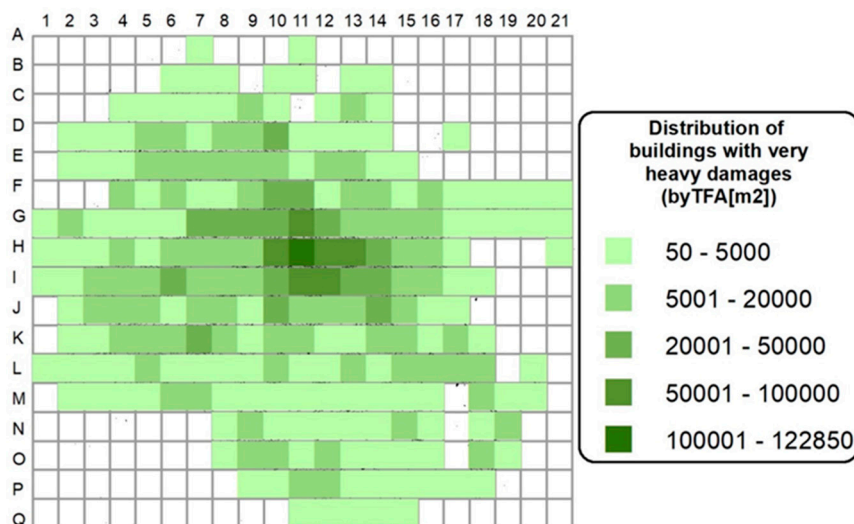


Figure 16. Distribution of buildings with very heavy damages—TFA [m<sup>2</sup>].

In assessing consequences, it is very important to know the distribution of unusable and demolished buildings to plan the restoration work volume in advance. Table 5 summarizes the results.

Table 5. Distribution of unusable and demolished buildings (by number and TFA).

Unusable buildings (number)	4128
Unusable buildings (TFA [m <sup>2</sup> ])	1,545,618
Demolished buildings (number)	1835
Demolished buildings (TFA [m <sup>2</sup> ])	434,137

### 3.1.2. Assessment of Social and Economic Losses

An essential aspect of assessing the consequences of strong earthquakes is the calculation of social losses, since human life is generally priceless. The most victims are observed in the event of a given building’s total structural collapse. The most important factors affecting social losses are the number of people per square meter and occupation during the earthquake (day or night).

Sofia's population amounts to 1,388,995 people according to data from the National Statistical Institute (31 December 2022). The occupancy of a city is estimated based on the number of people living in it (from national statistics) and the total built-up area; meanwhile, the number of victims and injured is calculated according to the well-known formulas of Coburn and Spence [26].

The results of the above calculations are available in two variants, depending on whether the earthquake occurs during the day or at night. Table 6 summarizes our study's results regarding social losses, i.e., the distribution of people affected, encompassing both injured and victims.

**Table 6.** Distribution of affected people—injured and victims (day and night).

Injured—By Day (Number)	Victims—By Day (Number)	Injured—By Night (Number)	Victims—By Night (Number)
6503–7227	1965–2184	26,020–28,913	7865–8739

The economic losses due to direct physical damage and destruction are instead estimated through the probability matrices of damage, whereby the economic damage index (DI) for a group of buildings is determined as the ratio of the total restoration cost to the value of all buildings in the group. In the end, representative values are obtained [24], which are given in Table 7.

**Table 7.** Representative DI values for different damage grades.

Damage Grade	1	2	3	4	5
DI	0.01	0.1	0.4	0.8	1

The economic losses in our study were calculated based on the results obtained for the damage and destruction of the buildings in question, amounting to EUR 4,222,426,000.

#### 4. Conclusions

The results of this study presenting the first risk assessment for the whole city of Sofia, are summarized below.

Estimating Sofia's deterministic seismic scenario is a key step in its seismic risk assessment, showing the highest intensity (up to 8.7 MSK) by the northern margin of the Vitosha Mountain. The generated scenario map is reliable and can be used for developing risk scenarios.

The number of completely destroyed buildings is 1835, which is 0.64% of the total built-up area. The most severely damaged buildings (heavy and very heavy damage) cover 7.93% and 3.00% of the total area, with the most significant damage being observed where the oldest low-rise buildings are located.

The social losses are time dependent, with 8 thousand victims 28 thousand injured for a night-time earthquake.

The economic losses (only from direct damage and destruction of the building stock) for the entire city are estimated at around EUR 4.22 billion.

This study's general conclusion is that Sofia is located in an area characterized by a high seismic risk, with considerable consequences in the case of a strong seismic event. The results show significant damage to many buildings, and large social and economic losses. The most significant damage is observed in those parts of the city where the oldest low-rise buildings are located. In these areas there is a combination of two factors. The first one is the presence of old buildings with higher vulnerability and the second is the very high seismic intensity ( $I = 8.6$  to  $I = 8.8$ ) in these parts of the city.

Most active human actions to reduce seismic risk depend on a state's economic potential, specifically its funds for creating and maintaining earthquake preparedness and overcoming their consequences.

Experiences in seismically active areas such as Bulgaria show that seismic risk can be reduced through effective urban planning, in accordance with the natural features and available structure of a settlement. This involves anti-seismic constructions and increasing people's preparedness to overcome the consequences of strong earthquakes via adequate preventive measures, population training, rescue activity planning, and active communication between science and all government levels.

The results in this study are very useful for Sofia's municipal authorities and, more specifically, rescue teams' priority planning of equipment and resources for natural disaster response plans.

**Author Contributions:** Conceptualization, D.E.S., D.S., S.S. and P.R.-T.; methodology, D.E.S. and D.S.; software, D.E.S.; validation, D.S., S.S. and P.R.-T.; formal analysis, D.E.S., D.S., S.S. and P.R.-T.; investigation, D.E.S. and D.S.; resources, S.S. and P.R.-T.; data curation, S.S. and P.R.-T.; writing—original draft preparation, D.E.S., D.S., S.S. and P.R.-T.; writing—review and editing, D.E.S., D.S., S.S. and P.R.-T.; visualization, D.E.S., D.S. and P.R.-T.; supervision, D.E.S., D.S. and S.S.; project administration, D.E.S.; funding acquisition, D.E.S. All authors have read and agreed to the published version of the manuscript.

**Funding:** This work was carried out in the framework of the National Science Program “Environmental Protection and Reduction of Risks of Adverse Events and Natural Disasters”, approved by the Resolution of the Council of Ministers № 577/17.08.2018 and supported by the Ministry of Education and Science (MES) of Bulgaria (agreement № D01-27/06.02.2024).

**Data Availability Statement:** Seismograms used in this study were collected using a classified network of the National Institute of Geophysics, Geodesy and Geography—BAS. (1980), National Seismic Network of Bulgaria and cannot be released to the public. Data can be obtained from Solakov et al. (2020)—Catalogue of the earthquakes in Bulgaria and surroundings since 1981, National Institute of Geophysics, Geodesy and Geography—BAS, at <https://doi.org/10.34975/ctlg-2020.v.1>. The classification of the building stock was carried out based on information from the Bulgarian state Geodesy, cartography, and cadastre agency.

**Conflicts of Interest:** The authors declare no conflicts of interest. The funders had no role in the design of the study; in the collection, analyses, or interpretation of data; in the writing of the manuscript; or in the decision to publish the results.

## References

1. Popov, A.; Toncheva, E.; Drosneva, E.; Boyadjiev, K.; Vacheva, K.; Vaklinova, M.; Tsonev, M. *Sofia—120 Years of Capital*; Prof Marin Drinov Publishing House of BAS: Sofia, Bulgaria, 1999; p. 267. (In Bulgarian)
2. Petkov, I.; Christoskov, L. On seismicity in the region of the town of Sofia concerning the macroseismic zoning. *Ann. Sofia Univ.* **1965**, *58*, 163–179.
3. Faccioli, E.; Pessina, V.; Pitilakis, K.; Ordaz, M. WP2: *Basis of a Handbook of Earthquake Ground Motions Scenarios. An Advanced Approach to Earthquake Risk Scenarios with Applications to Different European Towns*; Contract: EVK4-CT-2000-00014. 2003; p. 93.
4. Faccioli, E. Seismic hazard assessment for derivation of earthquake scenarios in Risk-UE. *Bull. Earthq. Eng.* **2006**, *4*, 341–364. [[CrossRef](#)]
5. Jackson, J.; McKenzie, D. The relationship between plate motions and seismic moment tensors, and the rates of active deformation in the Mediterranean and Middle East. *Geophys. J.* **1988**, *93*, 45–73. [[CrossRef](#)]
6. Solakov, D.; Simeonova, S.; Trifonova, P.; Georgiev, I.; Raykova, P.; Metodiev, M.; Aleksandrova, I. *Building Seismic Risk Management*; Part 2: Regional Seismotectonic Model and Model of Seismic Sources; Prof Marin Drinov Publishing House of BAS: Sofia, Bulgaria, 2019; pp. 21–45. (In Bulgarian)
7. Medvedev, S.; Sponheuer, W.; Kärnik, V. *Seismic Intensity Scale Verson MSK64 by UNESCO/NS/SEISM/28*; Paris, France. 1965; p. 7.
8. Watzof, S. *Earthquakes in Bulgaria During XIX Century*; Central Meteor. Station, Imprimerie de l'Etat: Sofia, Bulgaria, 1902; p. 93. (In Bulgarian and French).
9. Simeonova, S.; Solakov, D.; Aleksandrova, I.; Raykova, P.; Protopopova, V. The 2012 Mw5.6 earthquake in Sofia seismic zone and some characteristics of the aftershock sequence. *Bulg. Chem. Commun.* **2015**, *47*, 398–405.

10. Solakov, D.; Simeonova, S.; Raykova, P.; Aleksandrova, I. ANALYSIS OF SEISMICITY IN SOFIA SEISMOGENIC ZONE. In Proceedings of the 20th International Multidisciplinary Scientific GeoConference SGEM, Sofia, Bulgaria, 18–24 August 2020; Volume 20, pp. 435–442, ISBN 978-619-7603-05-7. [CrossRef]
11. Basili, R.; Kastelic, V.; Demircioglu, M.B.; Garcia Moreno, D.; Nemser, E.S.; Petricca, P.; Sboras, S.P.; Besana-Ostman, G.M.; Cabral, J.; Camelbeeck, T.; et al. The European Database of Seismogenic Faults (EDSF) compiled in the framework of the Project SHARE. 2013. Available online: <https://edsf13.ingv.it/> (accessed on 5 November 2024).
12. Worden, C.B.; Wald, D.J.; Sanborn, J.; Thompson, E.M. Development of an open-source hybrid global Vs30 model. In Proceedings of the Seismological Society of America Annual Meeting, Pasadena, CA, USA, 21–23 April 2015.
13. Abrahamson, N.; Silva, W.; Kamai, R. Summary of the ASK14 ground motion relation for active crustal regions. *Earthq. Spectra* **2014**, *30*, 1025–1055. [CrossRef]
14. Akkar, S.; Sandikkaya, M.A.; Bommer, J.J. Empirical ground-motion models for point-and extended source crustal earthquake scenarios in Europe and the Middle East. *Bull. Earthq. Eng.* **2014**, *12*, 359–387. [CrossRef]
15. Boore, D.M.; Stewart, J.P.; Seyhan, E.; Atkinson, G.M. NGA-West 2 equations for predicting PGA, PGV, and 5%-damped PSA for shallow crustal earthquakes. *Earthq. Spectra* **2014**, *30*, 1057–1085. [CrossRef]
16. Campbell, K.W.; Bozorgnia, Y. NGA-West2 ground motion model for the average horizontal components of PGA, PGV, and 5%-damped linear acceleration response spectra. *Earthq. Spectra* **2014**, *30*, 1087–1115. [CrossRef]
17. Chiou, B.S.J.; Youngs, R.R. NGA model for the average horizontal component of peak ground motion and response spectra. *Earthq. Spectra* **2014**, *30*, 1117–1153. [CrossRef]
18. Cauzzi, C.; Faccioli, E.; Vanini, M.; Bianchini, A. Updated predictive equations for broadband (0.01–10 s) horizontal response spectra and peak ground motions, based on a global dataset of digital acceleration records. *Bull. Earthq. Eng.* **2015**, *13*, 1587–1612. [CrossRef]
19. Scherbaum, F.; Delavaud, E.; Riggelsen, C. Model Selection in Seismic Hazard Analysis: An Information-Theoretic Perspective. *Bull. Seismol. Soc. Am.* **2009**, *99*, 3234–3247. [CrossRef]
20. Luzi, L.; Puglia, R.; Russo, E.; D’Amico, M.; Felicetta, C.; Pacor, F.; Lanzano, G.; Çeken, U.; Clinton, J.; Costa, G.; et al. The Engineering Strong-Motion Database: A Platform to Access Pan-European Accelerometric Data. *Seismol. Res. Lett.* **2016**, *87*, 987–997. [CrossRef]
21. Delavaud, E.; Scherbaum, F.; Kühn, N.; Allen, T. Testing the Global Applicability of Ground-Motion Prediction Equations for Active Shallow Crustal Regions. *Bull. Seismol. Soc. Am.* **2012**, *102*, 707. [CrossRef]
22. Nikolov, H.; Atanasova-Zlatareva, M. Establishing the surface deformation in the Sofia valley by means of SAR data. In *Proceedings of the International Workshop on Geosciences in Active Areas (WGAAL2023) Arrecife, Lanzarote, Canary Islands, Spain, 16–20 October 2024*, Servicio de Publicaciones del Cabildo Lanzarote 2024; (IGEO) Books and Parts of Books; Sampedro, J.A., Emilio, J., Herranz, H., Eds.; Servicio de Publicaciones del Cabildo de Lanzarote: Madrid, Spain, 2024; pp. 34–40. ISBN 978-84-128033-6-5. [CrossRef]
23. Atanasova, M.; Nikolov, H. APPLICATION OF SAR DATA TIME SERIES FOR MONITORING OF GEODINAMIC PROCESSES IN THE SOFIA REGION. In Proceedings of the 23th International Multidisciplinary Scientific GeoConference SGEM, Albena, Bulgaria, 3–9 July 2023; Volume 23, pp. 283–290. [CrossRef]
24. Simeonov, S.; Solakov, D.; Georgiev, I.; Vaceva, R.; Dimitrov, D.; Stefanov, D.; Simeonova, S.; Trifonova, P.; Vaseva, E.; Cherkezova, E.; et al. *Methodology for Analysis, Evaluation and Mapping of Seismic Risk of the Republic of Bulgaria*; Ministry of Regional Development and Public Works, Construction and Architecture: Sofia, Bulgaria, 2018; p. 132. (In Bulgarian)
25. Grünthal, G. (Ed.) *European Macroseismic Scale 1998 (EMS-98)*; Centre Européen de Géodynamique et de Séismologie: Luxembourg, 1998; p. 99. [CrossRef]
26. Coburn, A.; Spence, R. *Earthquake Protection*, 2nd ed.; John Wiley & Sons Limited: Hoboken, NJ, USA, 2002. [CrossRef]

**Disclaimer/Publisher’s Note:** The statements, opinions and data contained in all publications are solely those of the individual author(s) and contributor(s) and not of MDPI and/or the editor(s). MDPI and/or the editor(s) disclaim responsibility for any injury to people or property resulting from any ideas, methods, instructions or products referred to in the content.